

A Method for Measuring Powder Bed Density in Binder Jet Additive Manufacturing Process and the Powder Feedstock Characteristics Influencing the Powder Bed Density

A.M. Elliott*, P. Nandwana*, D. Siddel*, B. G. Compton†

*Manufacturing Demonstration Facility, Oak Ridge National Laboratory, 1 Bethel Valley Road,
Oak Ridge, TN 37830

†Department of Mechanical, Aerospace and Biomedical Engineering, University of Tennessee,
Knoxville, TN 37996

Abstract

Powder bed additive manufacturing involves layer-by-layer spreading of powders before melting, sintering or binding them. Traditionally apparent and tapped density measurements have been carried out to get an estimate of the powder bed density. Powder bed density is especially important in the case of binder-jet additive manufacturing where sintering is carried out as one of the steps to achieve full densification. During densification, shrinkage occurs. The extent of shrinkage depends upon the powder bed density. Thus, it is important to understand the role of powder feedstock on controlling the powder bed density. In the present paper, we have developed a technique to measure the powder bed density. We also used different powder feedstock materials to understand the role of powder size distribution and morphology on the powder bed density. The detailed results are presented.

This manuscript has been authored by UT-Battelle, LLC under Contract No. DE-AC05-00OR22725 with the U.S. Department of Energy. The United States Government retains and the publisher, by accepting the article for publication, acknowledges that the United States Government retains a non-exclusive, paid-up, irrevocable, worldwide license to publish or reproduce the published form of this manuscript, or allow others to do so, for United States Government purposes. The Department of Energy will provide public access to these results of federally sponsored research in accordance with the DOE Public Access Plan (<http://energy.gov/downloads/doe-public-access-plan>).

Introduction

Binder jet additive manufacturing (AM) is a versatile powder bed based AM technique that uses a counter-rotating roller to spread a powder bed. The next step involves selectively depositing a binder to adhere the powder particles together. In the following step, the build table is lowered and the powder piston is raised before the process is repeated. Figure 1 shows a schematic for the process. Once the part is printed, the green part is either subjected to infiltration or sintering to achieve full densification.

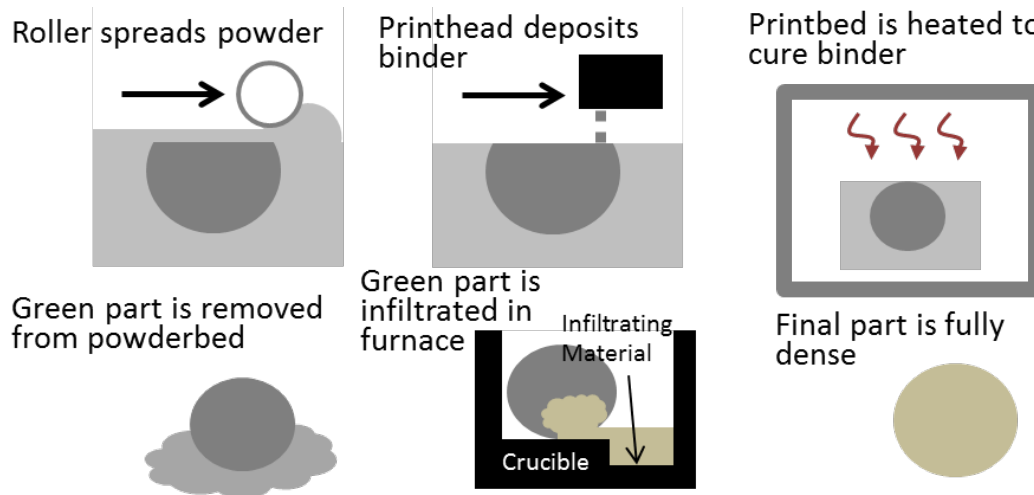


Figure 1 The process steps for binder jet additive manufacturing

The biggest issue with sintering of binder jet AM parts is the shrinkage associated with densification that results in warping and loss of dimensional tolerance. In order to predict and control shrinkage, the understanding of powder bed density is an important factor. The powder bed density directly translates to the density of the green part. A higher green density ensures reduced shrinkage during densification. As an example, a compact with a green density of 60% would shrink by 40% (the volume fraction of the pores) during full densification. On the other hand, an increase in green density to about 75% will result in about 25% shrinkage.

In the present paper, we demonstrate a methodology to measure the bed density of powder bed in binder jet AM. We use feedstock material with varying powder size distribution, shape and chemistry to determine the role of feedstock on powder bed density. Conventionally powder characterization involves conducting apparent and tap density measurements. However, we found that these measurements cannot be directly translated to determine the powder bed density. The detailed results are discussed in the subsequent sections.

Methods

Inconel 625 and Inconel 718 powders were acquired from different vendors. Powder size distribution (PSD) measurements were carried out using a Horiba LA 950 Laser Interferometer. Figure 2 shows the powder size distribution of the different feedstock materials.

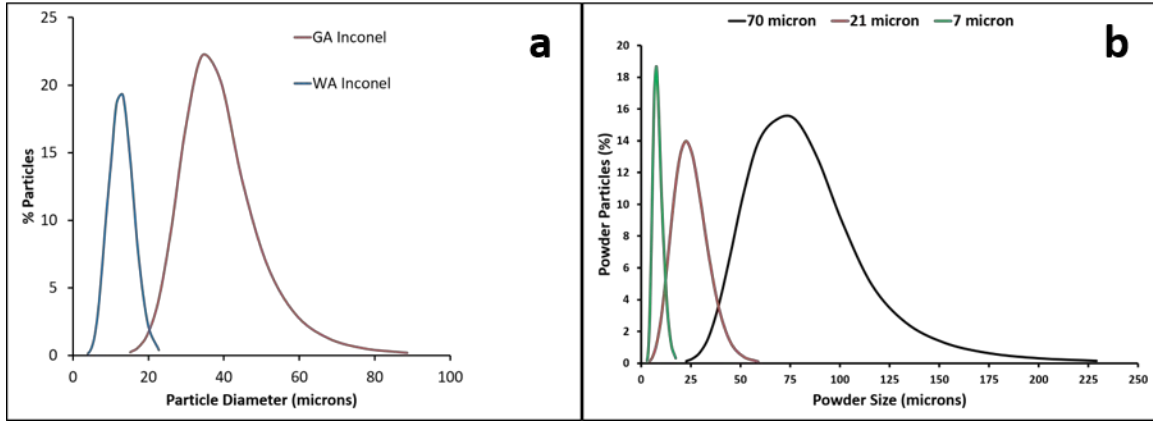


Figure 2 The powder size distribution of (a) gas and water atomized Inconel 625 powders, and (b) three different Inconel 718 powders

Powder morphology is presented in the micrographs in Figure 3. The secondary electron micrographs were acquired using a Hitachi S3400 scanning electron microscope. The powders will be referred by their average particle sizes.

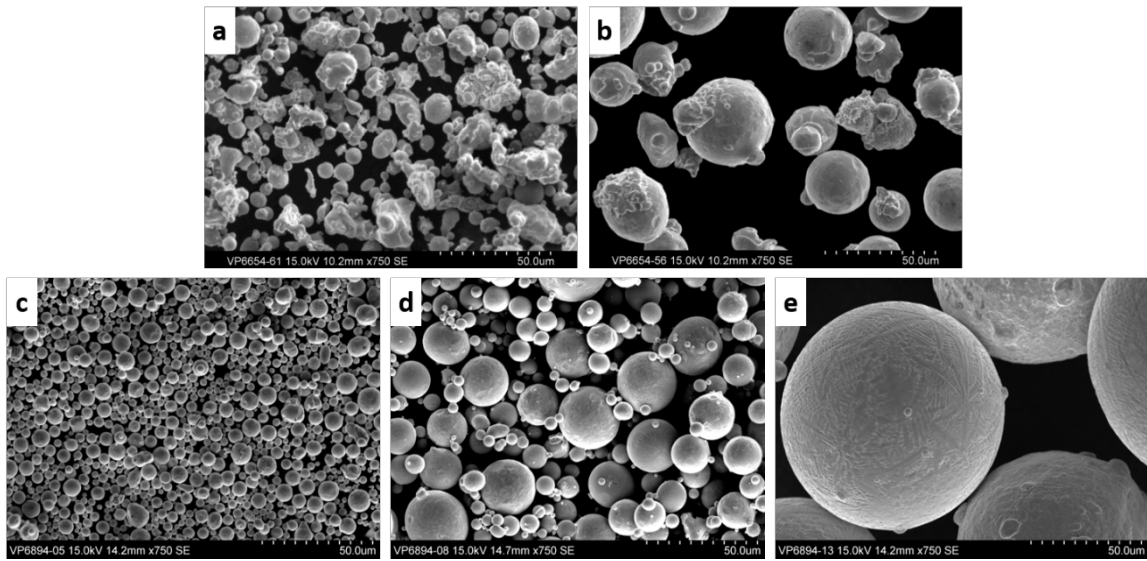


Figure 3 Secondary electron micrographs showing (a) irregular shaped water atomized Inconel 625 powders, (b) spherical gas atomized Inconel 625 powders, (c) 7µm Inconel 718 powders, (d) 21µm Inconel 718 powders, and (e) 70µm Inconel 718 powders.

Table 1 Average size and qualitative morphology of the powders for different feedstock material.

Material	Average Particle Diameter (μm)	Morphology (Qualitative)
Inconel 625	11	Angular
Inconel 625	35	Spherical
Inconel 718	7	Spherical
Inconel 718	21	Spherical
Inconel 718	70	Spherical

An X1-Lab binder jet system developed by Ex-One was used to fabricate the density cup samples. The density cups were cylinders with a diameter and height 10 mm and wall thickness 2mm. To deposit the cups, a counter rotating roller deposited a homogeneous powder bed but binder was deposited only along the cup contours, thus leaving loose powder in the cavity. After printing, the cups were removed, weighed, and then re-weighed after removing the loose powder to determine the weight of the loose powder. The dimensions of the cup were based on the computer aided design (CAD) file since no standards exist to measure fragile, concave parts such as these with sufficient accuracy. The cups were inverted and gently tapped once to extract the loose powder. Figure 4 shows an example of the cups used in the study. The apparent and tapped densities were measured in accordance with ASTM B213 and ASTM B527. The density of the powder bed as measured using the density cups will be referred to as powder bed density.



Figure 4 The density cups used for measurement of powder bed density.

Results and Discussion

Figure 5 shows the plot comparing the apparent, tapped and powder bed densities for the different feedstock materials used in the study. It is evident that the powder bed density is typically between the loose and tapped density values in all cases but one. In an earlier report, Liu et al. had reported similar findings on powder bed in selective laser melting [1].

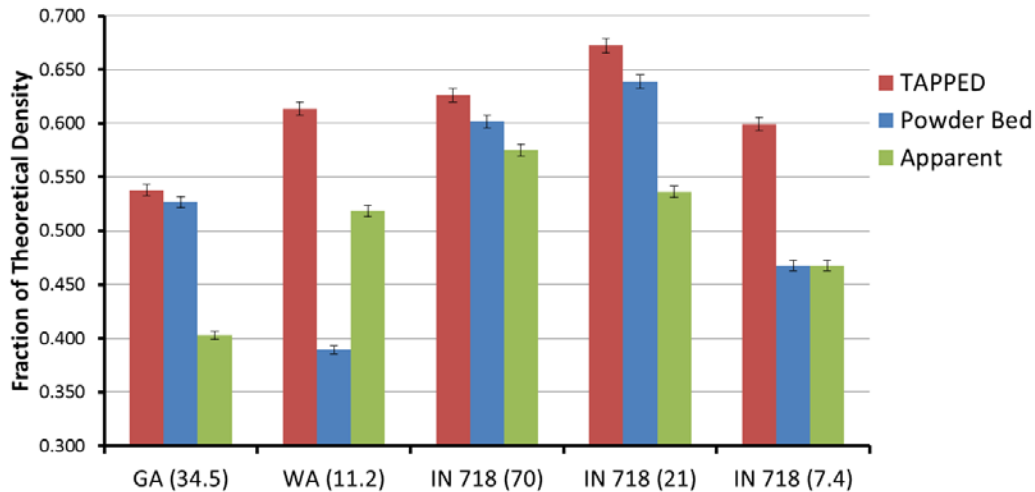


Figure 5 Plot of apparent, tapped and powder bed densities for different feedstock materials. The average powder sizes are mentioned in parentheses.

In the case of Inconel 625, the feedstock materials compared were water atomized powders with an average particle diameter $\sim 11 \mu\text{m}$ and gas atomized Inconel 625 with an average particle diameter $\sim 35 \mu\text{m}$. The $11 \mu\text{m}$ powders are the only feedstock material that has a powder bed density ($\sim 39\%$) that is less than the apparent and tap densities. These observations can be explained based on the fine size scale and irregular shape morphology of the powder particles as seen from Figure 3 (a). The jagged shape of the powder particles form interlocks between the particles. Abdullah and Geldart have discussed that angular particles have poorer packing compared to spherical particles [2]. In such a case, even the spreading characters will suffer since the powder has to also flow under the influence of the roller. The finer particles also have higher cohesive forces and can form agglomerates, which results in poorer packing fractions. This phenomenon has been discussed by Suri et al [3]. Thus, the water atomized $11 \mu\text{m}$ powders have a lower powder bed density compared to apparent and tapped densities.

For the $35 \mu\text{m}$ gas atomized spherical powders (Figure 3 b) the powder bed density is 98% of the tapped density. The relatively higher powder bed density can be explained on the basis of the spherical morphology and larger size compared to the water atomized particles. As a result of the low cohesive forces, the powders will spread better under the action of the roller and hence result in higher powder bed density values. Thus, one can conclude that to achieve higher green density, the feedstock material should have a spherical morphology and a larger particle size. A larger particle size may, however, have impeded sintering kinetics. Thus, an optimum powder size distribution should be used that can result in higher green densities along with faster sintering kinetics during post-processing.

For the Inconel 718 feedstock, all the powders were spherical in morphology as can be seen from Figures 3 (c, d, e). On comparing the powder densities, we observed that the $21 \mu\text{m}$ powders have the highest tapped and powder bed densities. In the case of apparent density, the powders follow the trend that's described in the literature [2, 4] that the finer the powders, the

poorer they pack due to high inter-particle frictional forces. The higher powder bed density of the 21 μm powders can be explained based on the observation by Liu et al. They showed that wider powder size distributions skewed towards the finer particle diameters result in higher bed densities [1]. Compared to the 7 μm powders, the 21 μm powders have a wider size distribution as can be seen from Figure 2 (b). Between 21 μm and 70 μm powders, the 70 μm powders have a wider size distribution but its tail end is skewed towards larger particle diameters that may be the possible reason for the 70 μm powders displaying 3% less density than the 21 μm powders.

Finally, the 21 μm powders have a particle size distribution similar to that of a bimodal distribution wherein the finer particles can occupy the voids between the larger powder particles resulting in higher density values for tapped and powder bed densities. The fines can be seen in Figure 3 (d). The 7 μm and 70 μm powders shown in Figures 3 (c) and (e) respectively do not have such smaller particles that can occupy the voids. Overall, it is difficult to correlate the observations between the Inconel 625 powders and Inconel 718 powders since the powders are expected to have different cohesive forces owing to their different chemical compositions.

Conclusions

The study presents a guideline towards the selection of appropriate powder feedstock to achieve high density green compacts. This is particularly important when the subsequent processing step involves sintering of the green compacts. Based on the study, the ideal size distribution should consist of particles with a d_{50} closer to $\sim 25 \mu\text{m}$ with a wider particle size distribution curve that is skewed at the tail end towards finer sizes. This size distribution would result in higher powder bed density as well as improved sintering kinetics during densification. The particle morphology should be spherical in order to achieve the maximum green density, thereby making gas atomized powder feedstock preferable over water atomized feedstock. Irregular powders will result in poor powder packing on the powder bed, that will subsequently result in very low powder bed densities ($\sim 39\%$ in case of water atomized Inconel 625). Such a large amount of porosity will significantly increase the shrinkage as well as the sintering time and may not reach full densification. Future studies need to be conducted to develop a theoretical framework to associate the powder size distribution with powder bed densities. Also, research needs to be carried out towards multimodal distributions to increase the green density of the as-deposited compacts.

Acknowledgements

Research was sponsored the U.S. Department of Energy, Office of Energy Efficiency and Renewable Energy, Advanced Manufacturing Office, under contract DE-AC05-00OR22725 with UT-Battelle, LLC. This research at the Oak Ridge National Laboratory's High Temperature Materials Laboratory was sponsored by the U.S. Department of Energy, Office of Energy Efficiency and Renewable Energy, Vehicle Technologies Program.

References

1. Bochuan Liu, Ricky Wildman, Christopher Tuck, Ian Ashcroft, Richard Hague, Solid Freeform Fabrication Symposium, 2011.
2. E.C. Abdullah, D. Geldart, Powder Technology (1999) 151-165.
3. Pavan Suri, Sundar V. Atre, Randall M. German, Jupiter P. de Souza, Materials Science and Engineering A356 (2003) 337-344.
4. A. Santomaso, P. Lazzaro, P. Canu, Chemical Engineering Science 58 (2003) 2857-2874.